Annals of Biomedical Engineering, Vol. 34, No. 5, May 2006 *(© 2006)* pp. 847–858
DOI: 10.1007/s10439-006-9114-8

Combined Transfer Function Analysis and Modelling of Cerebral Autoregulation

S. J. PAYNE and L. TARASSENKO

Department of Engineering Science, University of Oxford, Parks Road, OX1 3PJ, Oxford,

(Received 20 December 2005; accepted 15 March 2006; published online: 25 April 2006)

Abstract—The clinical importance of cerebral autoregulation has resulted in a significant body of literature that attempts both to model the underlying physiological processes and to estimate the mathematical relationships between clinically measurable variables, the most common of which are Arterial Blood Pressure and Cerebral Blood Flow Velocity. These approaches have, however, rarely been used together to interpret clinical data. A simple model of cerebral autoregulation is thus proposed here, based on a flow dependent feedback mechanism with gain and time constant that adjusts arterial compliance. Analysis of this model shows that it closely approximates a second order system for typical values of physiological parameters. The model parameters can be optimally estimated from available experimental data for the Impulse Response (IR), yielding physiologically reasonable values, although there is one free parameter that must be fixed. The effects of changes in feedback gain and time constant are found to be significant on the predicted IR and can thus be estimated robustly from experimental data. The effects of elevated baseline Intracranial Pressure (ICP) are found to be exactly equivalent to a reduced feedback gain, although the solution is much less sensitive to the former effect. A transfer function approach can be used to estimate autoregulation status clinically using a physiologically-based model, thus providing greater insight into the processes that govern cerebral autoregulation.

Keywords—Impulse response, Frequency response.

INTRODUCTION

The supply of nutrients to the brain and the removal of the waste products of cerebral metabolism are both crucial if cerebral function is to be maintained despite significant changes in physiological parameters such as Arterial Blood Pressure (ABP). Cerebral autoregulation has classically been taken to be the maintenance of Cerebral Blood Flow (CBF) in the face of varying Cerebral Perfusion Pressure (CPP), where CPP is the difference between ABP and Intracranial Pressure (ICP).[30] A failure of autoregulation is implicated in a variety of diseases, such as stroke and trauma.

The most widespread clinical variable is blood flow velocity, normally measured using Doppler Ultrasound over the middle cerebral artery (V_{MCA}). Since this measures blood velocity, the cross-sectional area of the vessel has to be assumed to remain constant for it to be a direct measure of flow rate.[25] It is also a measure of the flow into the cerebral system, rather than through the microvasculature.

Due to the importance of cerebral autoregulation, there has been considerable work performed to analyse its behaviour. This work can be approximately divided into two approaches. The former analyses the relationship between different clinical variables using a purely mathematical framework, such as transfer function analysis, making no physiological assumptions about the system. The latter relates the different clinical parameters using a physiologically-based model that can predict a range of variables, some that can be measured and some that cannot.

The only existing approach to attempt to bridge this gap is the popular model of autoregulation proposed by Tiecks.[25] It is based on the idea of an AutoRegulation Index (ARI), which can take any value between 0 and 9. 0 denotes no autoregulation, 9 the 'fastest' and 5 a 'normal' autoregulation. The model is based on a simple set of discrete equations, relating V_{MCA} to ABP, with parameters that are dependent upon the autoregulation gain, the damping factor and the time constant. The parameters, however, are not varied independently and no justification is given for their values.[10]

Transfer Function Analysis

Both linear and non-linear approaches have been used to determine the behaviour of the cerebral system where ABP and V_{MCA} are considered to be the input and output. Linear techniques characterise the system behaviour in terms of either the Impulse Response (IR),[14,18–20,31] which is equivalent to linear kernel analysis, or the Frequency Response (FR).[19,32] The non-linear methods have all been based on the use of non-linear kernels.[13] One of the advantages of linear kernel analysis is that any additional non-linear terms do not affect the linear analysis, since the linear and non-linear kernels are orthogonal.

The IR derived from normal subjects consistently shows undershoot, occurring at approximately 1–2 sec, of about one third of the initial value, returning to baseline quickly

with possible occasional slight overshoot. There is some difference between the results of individual studies, examples of which are shown in Fig. 1. A comprehensive study of seven of the most popular clinical tests, however, showed that the means of deriving the impulse response is unimportant.[21] The differences between studies thus seem to indicate a natural variation across the population.

The FR is characterised by three parameters: gain, phase and coherence. The squared coherence is a measure of the fraction of the output power that can be linearly related to the input power. Panerai[21] found that the gain increased with frequency in the range 0 to 0.5 Hz, whereas the phase was positive below 0.35 Hz, becoming slightly negative at higher frequencies. The coherence was high for frequencies above 0.2 Hz but low for frequencies below 0.1 Hz. Virtually identical results were obtained by other authors,[31, 32] who divided the frequency spectrum below 0.5 Hz into three regions:

1. Low frequency (<0.07 Hz): Low coherence, low gain and large phase lead.
2. Intermediate frequency (0.07–0.20 Hz): Increasing coherence, increasing gain and decreasing phase.
3. High frequency (>0.20 Hz): High coherence, relatively large gain and minimal phase lead.

Phase lead, corresponding to positive phase, indicates that V_{MCA} leads ABP. The only difference found is that in some studies the gain drops off slightly towards 0.5 Hz in Zhang's papers,[31,32] but in others it rises slightly.[19] However, this trend is small and difficult to identify clearly.

Similar results show a phase lead in the low frequency region,[1,4] as derived using a Cross-Correlation Function (CCF), calculated separately in each of the three frequency regions. The phase lead was shown to be greatest at low frequencies, decreasing as the frequency increased. Results presented by Narayanan[16] cover a wider range of frequencies, up to 1.5 Hz. Although the phase lead at low frequencies, decreasing as frequency increases, was again shown, the coherence was found to be somewhat higher than shown by Panerai.[19] The response of all three was found to be largely flat after 0.5 Hz up to the Nyquist frequency. A linear autoregressive with exogenous input (ARX) model has been found to predict the step response accurately,[12] whilst an autoregressive-moving average (ARMA) model based on the AutoRegulation Index (ARI), outlined above was used for a group of 14 healthy subjects.[22]

A more wide-ranging study[23] examined the V_{MCA}/ABP transfer function for both spontaneous oscillations around 0.1 Hz and deep breathing for 168 patients with severe carotid stenosis or occlusion. The spontaneous oscillations are thought to be caused by central oscillations in sympathetic nervous outflow[15] and are a naturally occurring feature of ABP. The results presented for the two conditions exhibit similar characteristics to those described above, although the coherence is very high for frequencies higher than 0.1 Hz.

There are thus a number of characteristics of the cerebral autoregulation system that seem to be widely agreed upon. However, it should be noted that the frequency bands used by different authors quoted above are very approximate, being likely to vary widely from subject to subject, and do not necessarily correlate to underlying physiological processes, such as respiration. The bands quoted are used simply to illustrate the characteristic behaviour of the system behaviour. In addition, the difficulty with analysing the FR is that any non-linearities in the signal make it difficult to interpret: the IR has the advantage that the linear component can be estimated independently of the non-linear components: it is thus a more robust way of examining the system behaviour.

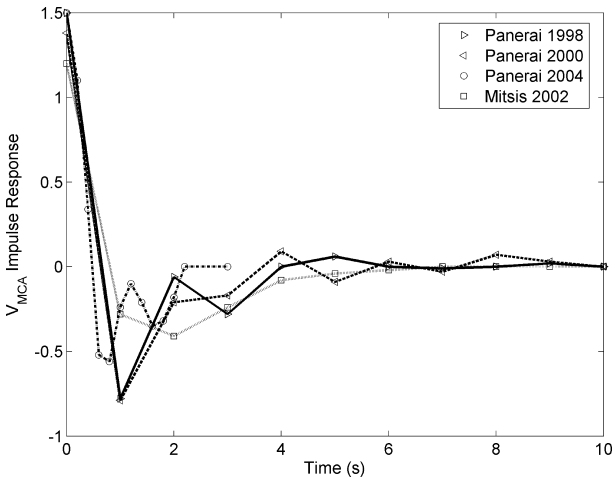

FIGURE 1. Impulse Responses for V_{MCA} derived by Panerai *et al.*, 1998, Panerai *et al.*, 2000, Panerai, 2004, and Mitsis *et al.*, 2002b.

Physiologically-Based Models

There is a large number of physiologically-based models available in the literature that attempt to characterise the behaviour of the cerebral autoregulation system. One simple model[10] assumes that there is a single simple flow-dependent feedback process with gain and delay. The resulting transfer function provides an accurate simulation of many of the features shown by the cerebral autoregulation system, but the phase lead found in experimental data at low frequencies is missing.

Another very simple physiological model[17] combines all the elements of the autoregulation system into three equivalent electrical components: two resistors and one capacitor, with values that vary with time. Although these can be adjusted to fit the experimental data well, it is difficult to interpret the parameter values in terms of physiological processes. A biphasic response is found, indicating that there is more than one time constant governing the

system behaviour, i.e. that the system is at least second order.

The model by Czosnyka[6] is a more detailed attempt to provide a hydrodynamic equivalent of the blood flow through the skull, through an analogous electrical circuit. Although the model structure is relatively simple, the components in the circuit are mostly non-linear and there is little information on some of the parameters, which makes this model difficult to use for analysis. Several similar models have been proposed by Ursino and co-workers.[27–29] These models differ in complexity, having either one or two autoregulating compartments with different feedback mechanisms, based either on flow or pressure.

Since the aim of this paper is to interpret the available experimental data and to investigate whether it can be used to gain information about the behaviour of cerebral autoregulation, we propose below a very simple model of autoregulation. The model is analysed and its IR derived and compared to the available experimental data. The aim of the work presented in this paper is two-fold: to illustrate how the two different approaches to examining the cerebral autoregulation system, as outlined above, can be combined by theoretical analysis of a physiologically-based model, and to use this analysis to investigate whether the status of autoregulation can be differentiated between subject groups.

MODEL

Model Equations

The haemodynamic model proposed here is shown in Fig. 2, using the well-established system of equivalents between hydrodynamic and electrical circuits. The arterial compartment is divided into regulating and non-regulating compartments: the first segment (R_{la}) represents the larger arteries down to, but excluding, the large pial arteries; the second (R_{sa}) the smaller arteries and arterioles, this segment being sub-divided into two as arterial compliance (C_a) is included to allow for changes in arterial volume. The division of the arterial compartment into two represents the fact that it is primarily the smaller arteries and arterioles that regulate most actively: the first segment is thus assumed to have a fixed resistance and blood volume, whereas the second has varying resistance and volume.

The capillaries are assumed to have a fixed resistance and volume, whereas the venous compartment is assumed to change in volume, as shown in Fig. 1, but to have a fixed resistance to flow for simplicity. The venous compartment is thus modelled as two resistors with a venous compliance (C_v) between. To simplify the model, the first of these resistances, representing the smaller veins, is combined with the capillary resistance to give R_{sv}, the second segment (R_{lv}) representing the larger veins. ICP is assumed constant here, since the time constants that govern ICP are significantly different from those of autoregulation. The effects of changes in baseline ICP are investigated below.

It should be noted that changes in capillary compliance and resistance can play an important role in certain clinical conditions. For reasons of simplicity, this effect is not considered here, but would be a necessary addition to the model under these conditions, which include stroke and which can lead to hypoxic foci and cortical spreading depression, amongst other effects.

The arterial volume is assumed to comprise a fixed quantity, corresponding to the non-regulating vessels, V_{la}, and a varying quantity, corresponding to the regulating vessels, V_{sa}:

$$V_a = V_{\mathrm{la}} + V_{\mathrm{sa}}. \tag{1}$$

Since vessel resistance is proportional to the inverse of radius to the power four and volume is proportional to the radius squared, for a given vessel length, volume varies according to the inverse square root of the resistance:

$$\frac{V_{\mathrm{sa}}}{\overline{V_{\mathrm{sa}}}} = \sqrt{\frac{\overline{R_{\mathrm{sa}}}}{R_{\mathrm{sa}}}}, \tag{2}$$

if it is assumed that regulating vessels constrict and dilate uniformly over their length. Vasoconstriction and

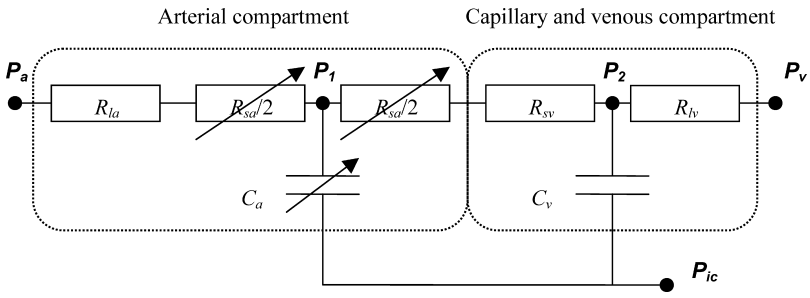

FIGURE 2. Schematic of model. P_{a}, systemic arterial pressure; R_{la}, resistance of non-regulating arterial compartment; P_1, R_{sa}, and C_{a}, pressure, resistance, and compliance of regulating arterial compartment; R_{sv}, resistance of capillary compartment and small veins; C_{v}, venous compliance; P_2, venous pressure; P_{v} and R_{lv}, venous pressure and resistance of large veins, respectively; P_{ic}, intracranial pressure.

vasodilation thus play an important part in the model response to changes in ABP. The overbar is used to denote baseline conditions throughout the paper.

From the definition of compliance, the rate of change of arterial volume can be related to the compliance and transmural pressure:

$$\frac{dV_a}{dt} = \frac{d\left(C_a\left(P_1 - P_{\text{ic}}\right)\right)}{dt}. \tag{3}$$

The key parameter in Eq. (3) is arterial compliance, since it is assumed that CBF regulation occurs through changes in arterial compliance, i.e. the properties of the arterial vessel walls. The equations for the change in venous volume are taken directly from Ursino,[29] where venous volume is related to changes in transmural pressure:

$$\frac{dV_v}{dt} = C_v \frac{d}{dt}(P_2 - P_{\text{ic}}), \tag{4}$$

and venous compliance, C_v, is assumed to be inversely proportional to transmural pressure:

$$C_v = \frac{1}{k_{\text{ven}}\left(P_2 - P_{\text{ic}} - P_o\right)}, \tag{5}$$

where k_{ven} and P_o are constants.

The pressures and volumes in the haemodynamic model can be calculated from conservation of volume at the relevant nodes:

$$\frac{dV_a}{dt} = \frac{P_a - P_1}{R_{\text{la}} + R_{\text{sa}}/2} - \frac{P_1 - P_2}{R_{\text{sa}}/2 + R_{\text{sv}}}, \tag{6}$$

$$\frac{dV_v}{dt} = \frac{P_1 - P_2}{R_{\text{sa}}/2 + R_{\text{sv}}} - \frac{P_2 - P_v}{R_{\text{lv}}}. \tag{7}$$

The regulation of CBF is assumed to be of the form:

$$\tau \frac{dx}{dt} = -x + G\left(\frac{q - \overline{q}}{\overline{q}}\right), \tag{8}$$

where a change in fractional CBF from its baseline value acts to stimulate a delayed change in the state variable x, with feedback gain G and time constant τ. CBF regulation is assumed to act on the microvascular CBF:

$$q = \frac{P_1 - P_2}{R_{\text{sa}}/2 + R_{\text{sv}}}. \tag{9}$$

The state variable is then assumed to change arterial compliance as:

$$C_a = \bar{C}_a\left(1 - x\right). \tag{10}$$

A linear relationship is assumed since only the linear behaviour of the system, and hence small changes, is examined here. Although feedback based directly on CBF is not truly physiologically plausible, it provides a simple feedback mechanism and has been found to simulate the expected behaviour of the autoregulation system well.[29] To simulate the true mechanisms, a more comprehensive model would be required, which is beyond the scope of this analysis.

Model Analysis

Since the experimentally derived IR of the cerebral system is obtained using small signal analysis, the model equations can be linearized about the baseline conditions to determine the predicted system behaviour. An outline of the derivation is given in Appendix A. The resulting system can be expressed in terms of the transfer functions relating either CBF or V_{MCA} to ABP. For the latter transfer function it is assumed that the vessel cross-sectional area is invariant with ABP and hence velocity fluctuations are solely related to change in flow. These transfer functions are expressed in terms of the Laplace transform variable, s, where CBF, V_{MCA} and ABP are given as fractional changes relative to their basal values:

$$\frac{\Delta q/\overline{q}}{\Delta p_a/\overline{p}_a} = H\left(s\right), \tag{11}$$

$$\frac{\Delta V_{\text{MCA}}/\bar{V}_{\text{MCA}}}{\Delta p_a/\bar{p}_a} = J\left(s\right), \tag{12}$$

where:

$$H\left(s\right) = \frac{1 + \alpha_1}{\beta_1\left(1 + \alpha_1\right) - \left(\beta_2 + \frac{\beta_3}{1 + s\tau_v}\right)\left(1 - \alpha_1 - s\alpha_1\tau_a\right) + \left(\frac{\alpha_2}{1 + s\tau}\right)\left(2 - s\alpha_1\tau_a\right)}, \tag{13}$$

$$J\left(s\right) = \frac{1}{\beta_1}\frac{\beta_1\left(1 + \alpha_1\right) + s\alpha_1\tau_a\left(\beta_2 + \frac{\beta_3}{1 + s\tau_v}\right) + \left(\frac{\alpha_2}{1 + s\tau}\right)\left(-s\alpha_1\tau_a\right)}{\beta_1\left(1 + \alpha_1\right) - \left(\beta_2 + \frac{\beta_3}{1 + s\tau_v}\right)\left(1 - \alpha_1 - s\alpha_1\tau_a\right) + \left(\frac{\alpha_2}{1 + s\tau}\right)\left(2 - s\alpha_1\tau_a\right)}, \tag{14}$$

and the relevant non-dimensional parameters and time constants are:

$$\alpha_1 = \frac{\bar{V}_a/\bar{q}}{\bar{R}_{\text{sa}}\bar{C}_a}, \tag{15}$$

$$\alpha_2 = G\left[\left(\frac{\bar{p}_a - \bar{p}_{\text{ic}}}{\bar{p}_a - p_v}\right) - \beta_1\right], \tag{16}$$

$$\beta_1 = \frac{R_{\text{la}} + \bar{R}_{\text{sa}}/2}{R_{\text{total}}}, \tag{17}$$

$$\beta_2 = \frac{\bar{R}_{\text{sa}}/2 + R_{\text{sv}}}{R_{\text{total}}}, \tag{18}$$

$$\beta_3 = \frac{R_{\text{lv}}}{R_{\text{total}}}, \tag{19}$$

$$\tau_a = \left(R_{\text{la}} + \bar{R}_{\text{sa}}/2\right)\bar{C}_a, \tag{20}$$

$$\tau_v = R_{\text{lv}}\bar{C}_v. \tag{21}$$

The first parameter is a ratio of time constants, the second a measure of feedback gain, the third to fifth the resistance fractions of the different parts of the compartmental model and the sixth and seventh are time constants related to the arterial and venous compartments respectively. ICP and venous outflow pressure are assumed constant. Although there are five non-dimensional parameters in the model, one is redundant, since $\beta_1 + \beta_2 + \beta_3 = 1$ and the total resistance is simply the sum of all the resistances in the model, relating the baseline values of blood pressure drop and flow rate.

The CBF transfer function has numerator and denominator of order 2 and 3 respectively, but that of the V_{MCA} has numerator and denominator both of order 3. The fact that they are of the same order is in agreement with Giller and Mueller.[9] The IR and FR will thus be different in shape as well as in magnitude, particularly at high frequencies, where the CBF transfer function will roll-off at 90° lag, whereas the V_{MCA} transfer function will plateau at zero phase. Note that the transfer functions for V_{MCA} and CBF are different, i.e. the former is not an exact marker for the latter.

Before comparing the transfer function with experimental data, it is helpful to consider whether the transfer functions can be simplified further, given typical values of the model parameters. It is known that the majority of the resistance to flow occurs in the arteries and arterioles, with the venous vessels presenting very little resistance to flow. If β_3 can thus be assumed to be close to zero, the transfer functions approximate to:

$$H(s) = \frac{1+\alpha_1}{\beta_1(1+\alpha_1) - (1-\beta_1)(1-\alpha_1 - s\alpha_1\tau_a) + \left(\frac{\alpha_2}{1+s\tau}\right)(2 - s\alpha_1\tau_a)}, \tag{22}$$

$$J(s) = \frac{1}{\beta_1} \frac{\beta_1(1+\alpha_1) + s\alpha_1\tau_a(1-\beta_1) + \left(\frac{\alpha_2}{1+s\tau}\right)(-s\alpha_1\tau_a)}{\beta_1(1+\alpha_1) - (1-\beta_1)(1-\alpha_1 - s\alpha_1\tau_a) + \left(\frac{\alpha_2}{1+s\tau}\right)(2 - s\alpha_1\tau_a)}. \tag{23}$$

The transfer functions are reduced in order by 1 in both numerator and denominator, making both systems second order. The number of parameters in the transfer function is also reduced to five ($\alpha_1, \alpha_2, \beta_1, \tau_a, \tau$). These five parameters uniquely define the coefficients of the V_{MCA} and CBF transfer functions.

Model Validation

To derive the V_{MCA} IR, the transfer function, $J(s)$, is written in a slightly different form:

$$J(s) = \frac{1}{\beta_1}\left[1 + \frac{(1-\beta_1)(1-\alpha_1) - 2\left(\frac{\alpha_2}{1+s\tau}\right)}{\beta_1(1+\alpha_1) - (1-\beta_1)(1-\alpha_1 - s\alpha_1\tau_a) + \left(\frac{\alpha_2}{1+s\tau}\right)(2 - s\alpha_1\tau_a)}\right]. \tag{24}$$

This is done to reduce the second term to one with numerator of order one less than the denominator: the first term is then a constant, giving an impulse at the origin in the time series. Since the first term is not considered in the experimentally-derived response, it is the second term that is fitted to the experimental data. There are thus only four free coefficients (due to arbitrary scaling between the numerator and denominator) that can be estimated from experimental data. Since there are five parameters in the model that determine the IR, there is one degree of redundancy in the model, which cannot be determined experimentally.

The IR in Eq. (24) was optimally fitted using least squares error to the experimental data of Mitsis.[14] This study was chosen as the intra-subject variation in experimental IR is small and it was based entirely on healthy subjects. This is also the case for other studies, which have slightly different IR, as shown in Fig. 1, but they all exhibit the same fundamental style of behaviour and the results obtained below are relatively insensitive to which data set is used.

The data of Mitsis was taken from 5 young healthy subjects. ABP was measured by finger photoplethysmography (Finapres, Ohmeda) and V_{MCA} by trans-cranial Doppler at 2 MHz for a period of 2 hr following 30 min of supine rest. Following sampling at 100 Hz, the waveforms were integrated over the cardiac cycle to give beat-to-beat values, which were finally resampled at 1 Hz.

The optimisation was performed using the 'fminsearch' routine in MATLAB, as this is based on the Nelder-Mead Simplex method and is highly robust. The optimisation routine was run many times for a wide range of initial values and convergence to the same error minimum was found every time, indicating the algorithm found the true global error minimum. In addition, following this optimisation, white noise was added to the values taken from Mitsis[14] to test the robustness of the parameter values calculated by the algorithm to small variations in the experimental IR: the results are presented below. Only the robustness of the algorithm in fitting the IR is considered here: the robustness of the method of determining the IR is not considered since it is a separate issue.

A range of fixed values of β_1 was used sequentially to investigate whether the quality of the model fit was strongly dependent upon the value of this parameter. The resulting optimal fit and experimental IR is shown in Fig. 3a, with the variation of the optimal values of the other model parameters withβ_1 shown in Fig. 3b. The RMSE (0.0145) is very low, indicating a very good fit to the data, and is the same for all fits. There is thus just one degree of freedom in the model, which determines all the other model parameters uniquely. The use of fixedβ_1 here is governed by the fact that the arterioles that control blood flow comprise most of the resistance to flow: it is thus likely to be very close to 0.5, since the remainder of the vascular resistance is relatively small. If a value of 0.5 is chosen, then the optimal values of the other parameters are:

$$\alpha_1 = 0.5613, \quad \alpha_2 = 0.2858, \quad \tau_a = 1.2424s, \quad \tau = 2.9974s.$$

White noise was added to the IR, as described above, 50 times with standard deviation 0.02 and the values of the

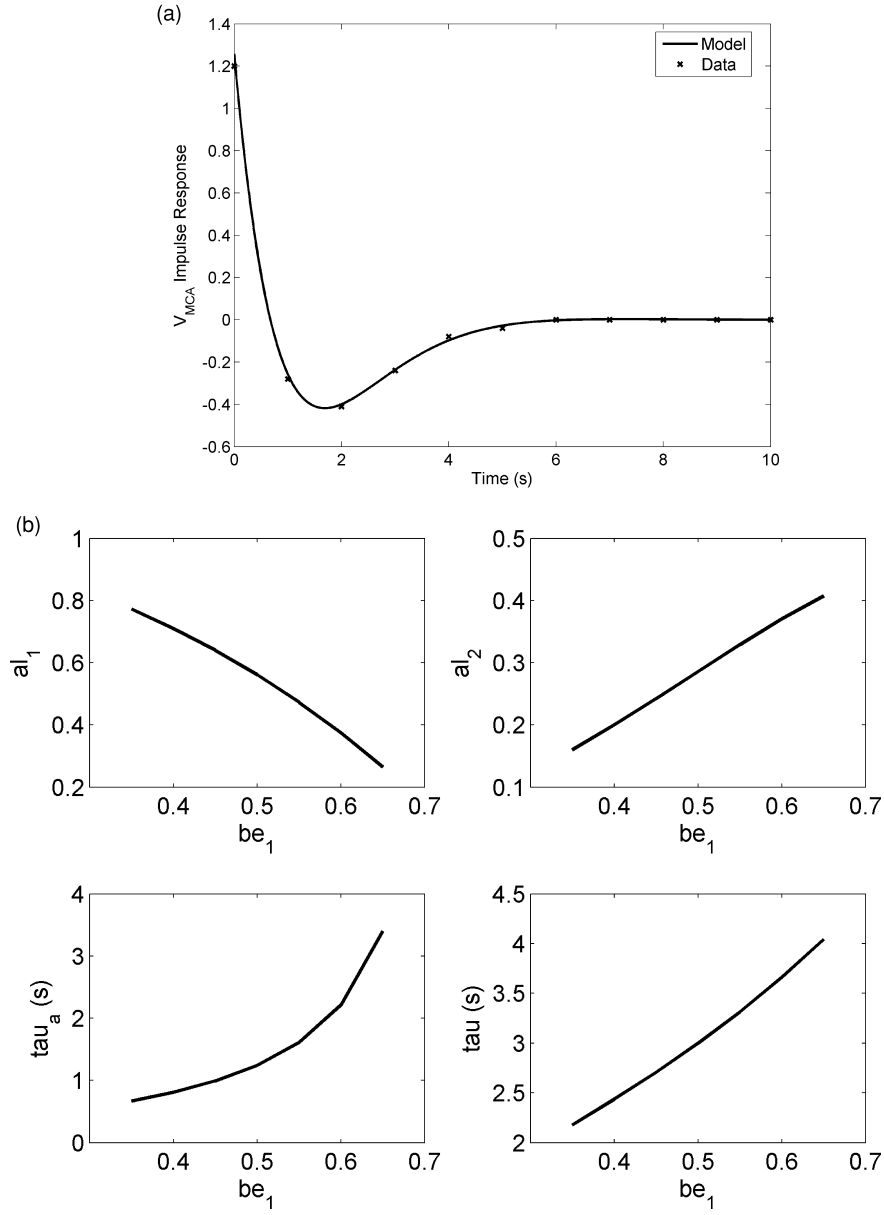

FIGURE 3. (a) Optimal model fit to experimental data for V_{MCA} IR from Mitsis *et al.*, 2002b; (b) Variation of the optimal values of the other model parameters with β_1 for optimal model fit.

parameters recalculated each time. 0.02 was chosen for the standard deviation since this gave a signal to noise ratio in the IR of approximately 1%. The standard deviations in the four parameter values were found to be 1.6, 6.6, 4.7 and 9.0% respectively. There is thus more robustness in the estimation of some of the model parameters than in others: in particular, α_1 is a robust estimate, whereas the others are somewhat less so. For higher values of noise on the IR, the variation in the estimate of the model parameters will clearly be larger. However, estimating the IR is a well-established technique and the algorithm used by Mitsis[14] is designed to be highly robust to noise, so the levels of noise on the IR should be very low.

The first calculated parameter, α_1, is the ratio of the arterial transit time to the time constant associated with the regulating arterial compartment. From experimental data,[11] baseline CBF and CBV are approximately 58 ml/100 g/min and 3.74 ml/100 g respectively, with arterial CBV approximately 23% of the total CBV at baseline. The arterial transit time is thus estimated to be 0.9 sec and the regulating arterial time constant can be estimated at 1.6 sec fromα_1. The value of τ_a of 1.24 sec can be used to estimate the ratio of non-regulating to regulating arterial resistance as 27.5:72.5%. This is a reasonable estimate, since the regulating arterioles comprise most of the arterial resistance, although it is difficult to compare its value to experimental data. Since

the non-dimensional gain term, α_2, contains a number of different variables, estimating the value of the feedback gain is difficult. In addition, since the feedback mechanism incorporated in the model here is very simple, attempting to characterise a number of processes within a single variable with gain and time constant, it is difficult to compare it directly to available data. However, more importantly, the effects of raised or lowered feedback gain can be examined, relative to the estimated baseline value, which will provide an insight into whether changes in the feedback processes for different subject groups can be determined experimentally.

To test this, the data of Panerai[18] for both a normal subject and a head injured patient was analysed using our proposed model. Since no information is given by Panerai about the data or its processing, only a comparison between the two IR is given, rather than the absolute values to illustrate the value of the proposed model. The value of α_1 is found to increase by 59% and the values ofα_2,τ_a andτ to decrease by 62, 69, 66% respectively. The large decrease in the non-dimensional gain term, α_2, is exactly as expected, since it has been shown by Ursino[29] that the feedback gain reduces in head injured patients. Impaired autoregulation can thus clearly be seen in the experimental IR.

The decrease in the time constants is perhaps somewhat surprising. The increase in the non-dimensional term, α_1, implies either a larger arterial transit time and/or a smaller time constant associated with the regulating arterial compartment. This non-dimensional approach does illustrate the difficulty of directly interpreting the results clinically, but the proposed model does provide substantially more information than has been previously available, by relating the parameters within a physiological model to the experimental IR.

Since the V_{MCA} IR has been modelled and optimally fitted to the experimental data, the CBF IR can directly be calculated, as shown in Fig. 4a (CBF IR is scaled to a maximum value of 1 for easier comparison: actual maximum value 4.4776). There are only very slight differences between the derived CBF IR as the parameters are optimised for different values of β_1, Fig. 4b: the CBF IR can thus be robustly estimated from the V_{MCA} IR. The CBF IR is noticeably different from the V_{MCA} IR, indicating that although V_{MCA} is a useful surrogate for microvascular CBF, there are significant differences in their behaviour. In particular, the CBF IR has a much higher initial value but much less undershoot, indicating that it is more heavily damped than the V_{MCA} IR.

The FR for both V_{MCA} and CBF are shown in Fig. 5. These both show that there is a flat response at low frequencies, slight resonance in the range approximately 0.01–1 Hz, where autoregulation is less effective, and then roll-off at high frequencies, like a low pass filter, for CBF, but a second plateau for V_{MCA}. The phase lead agrees with experimental data, which is only acquired at low frequencies, for which CBF leads ABP. At very low frequencies, the phase lead is predicted to drop back to zero: however, there are very few studies that have recordings of sufficient duration to explore these low frequencies. One of the few[32] seems to show that the phase lead drops at low frequencies, but the coherence also drops at these frequencies, making comparisons difficult. More detailed experimental data would be valuable in interpreting the frequency response in more detail. However, the proposed model seems to provide a good agreement with the available experimental data. It can thus be used to examine the effects of changes in the

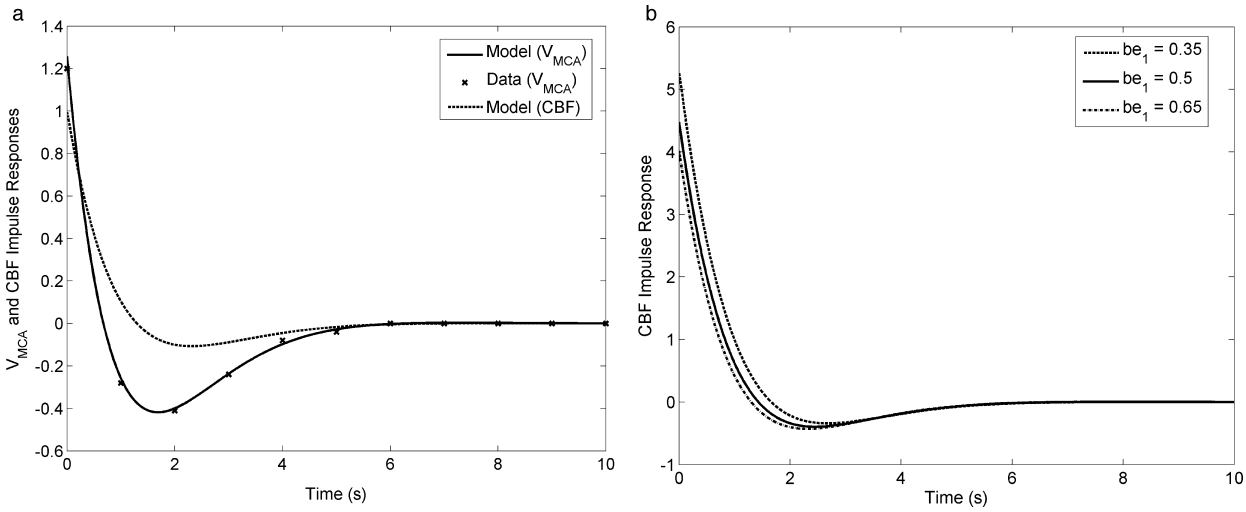

FIGURE 4. (a) CBF IR calculated from optimal model fit for V_{MCA} IR (scaled to a maximum value of 1 for easier comparison: actual maximum value 4.4776); (b) Variation in CBF IR for different β_1, each optimised separately.

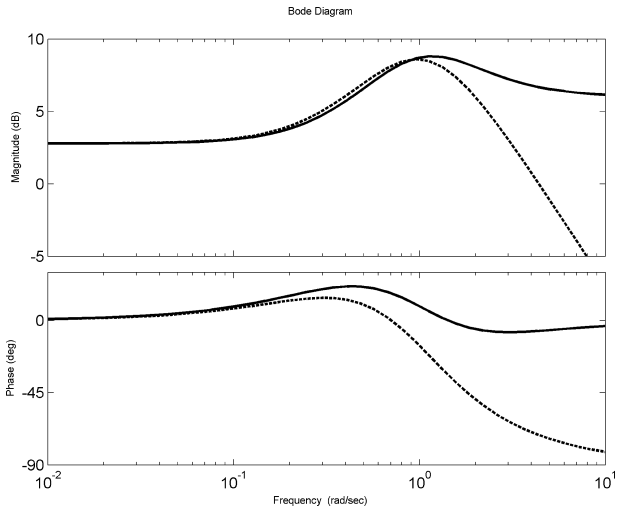

FIGURE 5. Frequency Response for both V_{MCA} and CBF, optimal model parameters.

system behaviour on the V_{MCA} IR, which will be important if the IR is to be of clinical use in investigating the status of cerebral autoregulation.

Model Predictions

The change in V_{MCA} IR as both the feedback gain and time constant are varied is shown in Figs. 6a and 6b respectively, assuming a value for β_1 of 0.5. As the feedback gain is elevated, the response becomes increasingly oscillatory, with a deeper trough occurring at a reducing time: the response is thus speeding up, but becoming less stable, as examined below. As the feedback time constant is elevated, the reverse response occurs, i.e. the response becomes faster as the time constant is reduced, as expected. The initial value of the IR is, however, invariant with feedback gain and time constant. This is a significant difference from the model of Tiecks,[25] Fig. 7, where the initial value decreases as autoregulation is impaired. From the initial value theorem and Eq. (24), this initial value is predicted here to be equal to$(1-\alpha_1)/\alpha_1\beta_1\tau_a = 1.2582$. Since the effects of variations in feedback gain and time constant are different, they can be estimated independently: the status of cerebral autoregulation can thus be estimated robustly from the available experimental data. The model of Tiecks, does predict that the magnitude of undershoot increases as ARI is raised, similar to the model proposed here: however, the advantage of our model is that the IR is directly related back to the feedback mechanisms through both feedback gain and time constant.

However, it is only strictly the non-dimensional gain parameter, α_2, that can be estimated from the experimental data, rather than the actual feedback gain, Eq. (16). The feedback gain is scaled by both a pressure and resistance ratio. If ICP is close to venous pressure, then the pressure ratio is close to one: however, if ICP is elevated, the non-dimensional parameter, α_2, is reduced. Conversely, if the feedback gain is estimated from the data but with an incorrect ICP, the actual gain, G, will be slightly inaccurate: a higher than expected ICP will result in an over-prediction of the gain and vice versa. The effects of changes in baseline ICP will thus be similar to those of changes in feedback gain, Fig. 6a. However, the parameter α_2 is much less sensitive to changes in ICP than feedback gain: an increase of 10% in feedback gain gives an IR exactly equivalent to one with an increase of 39% in ICP, using typical values of baseline pressure. Although the system response is thus determined by both the feedback gain and ICP, neither of which can be independently determined, since the response is much less sensitive to ICP, it is reasonable to take α_2 as a measure of feedback gain, except in subjects where ICP is known to be significantly altered.

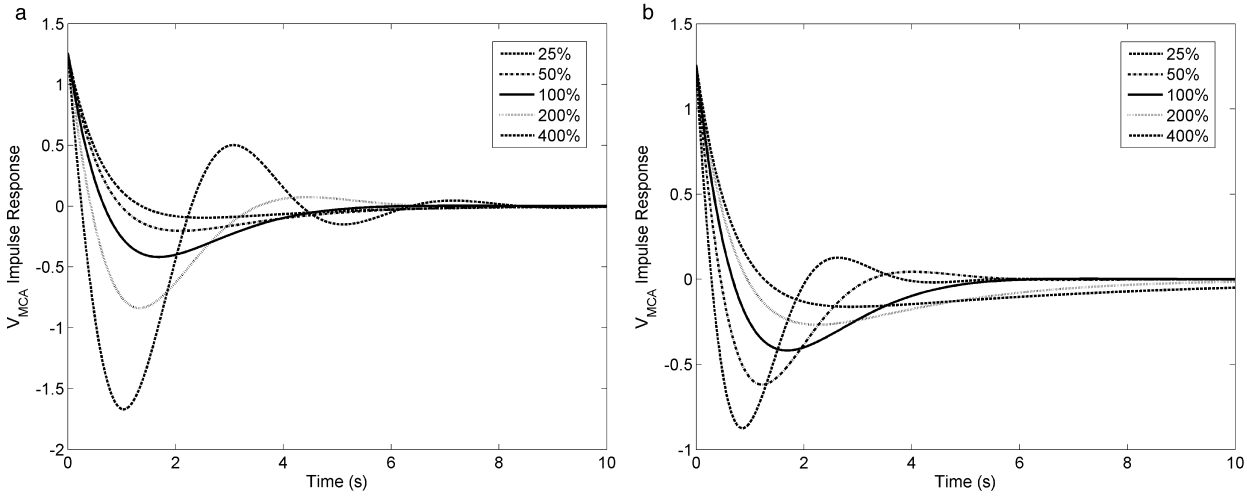

FIGURE 6. Variation in V_{MCA} IR for changes in: (a) feedback gain; and (b) feedback time constant.

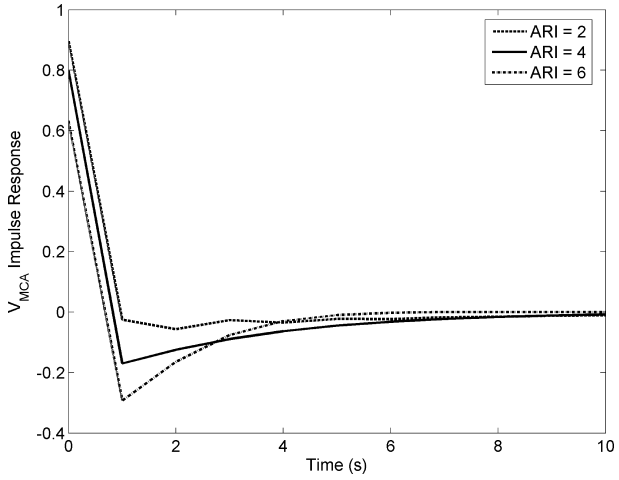

FIGURE 7. V_{MCA} IR predicted by model of Tiecks *et al.*, 1995.

One of the advantages of the simple model presented here is that the stability of the system can be examined analytically. Using a standard analysis[7] yields the following stability criterion in non-dimensional form:

$$\alpha_2 \leq (1-\beta_1) + \frac{\tau}{\tau_a}\left(1 - \left(\frac{1-2\beta_1}{\alpha_1}\right)\right). \qquad (25)$$

Since $\beta_1 \approx 1/2$, this reduces to:

$$\alpha_2 \leq \frac{1}{2} + \frac{\tau}{\tau_a}. \qquad (26)$$

For the values calculated earlier from the experimental data, the left hand side is equal to 0.56, whereas the right hand side is equal to 2.91. The model is thus well within the stable region, as would be expected. However, it can be seen that both the feedback gain and time constant determine the stability of the system. Changes in ICP will affect the stability, but significantly less than changes in feedback gain or time constant.

A similar model to the one here was proposed by Ursino[29] and used to fit experimental data recorded from 44 tracings from 13 different patients, all of whom had severe head injuries. If the components of the model that deal with the response to CO_2 challenges are neglected, only three model parameters were considered: CSF outflow resistance, intracranial elastance coefficient and autoregulation gain. The first two are not directly included in this model, as CSF flow and ICP dynamics are neglected, whereas the effect of the third on the model behaviour has already been considered in detail. However, in the Ursino model, baseline ICP is adjusted by changing CSF outflow resistance, which was found to vary widely across the patient group. The feedback gain also varied over an order of magnitude, with some subjects showing significantly impaired autoregulation. The effects of changes in ICP and feedback gain have been shown above not to have an independent effect on the system IR, so it is not possible to determine both of these directly from the IR unless ICP is measured. In addition, Ursino[26,29] did not consider the autoregulation time constant, which has been shown here strongly to influence the system behaviour.

It is somewhat surprising that the choice of feedback time constant has such an effect on the IR: the influence of feedback gain might be expected, but the influence of the time constant is less expected. A value of 20 sec was chosen by Ursino and Lodi,[27] since "the brain vessel autoregulation is quite fast, completing its action within 0.5–1 min from the beginning of a perfusion pressure change." The value of feedback gain is chosen by Ursino and Lodi[27] to "ensure that CBF remains quite constant within the autoregulation range." The values derived here are somewhat smaller, but the values quoted are somewhat of a compromise, attempting to encompass a number of different mechanisms within a single value. The excellent agreement that the model predictions have with the available experimental data indicates that the model is a reasonable one and that the estimates are of the correct magnitude under normal conditions: however, the impact on these feedback parameters of different pathological states cannot be assessed with the existing model. It would thus be highly worthwhile to attempt to relate the values of feedback gain and time constant to more detailed physiological models of the autoregulatory processes, since they have both been shown here to have a very significant effect on the system behaviour.

The effects of ageing or different pathological states on the IR have only been investigated by a few authors. One study[18] found that the IR had a smaller and earlier dip in a patient with severe head injuries in comparison with a normal subject. From Fig. 6, this would imply a larger feedback gain or a smaller time constant, neither of which is likely: however, since only one subject is considered, it is difficult to draw definite conclusions. The initial value of the IR was, however, found to be very similar, which would support the model proposed here, rather than that of Tiecks, although again this cannot be concluded with certainty since there is only one subject.

The dynamic behaviour of the cerebral autoregulation system as assessed through the use of ARI has been shown to be unaffected by ageing.[2] However, dynamic cerebral autoregulation was found to be impaired in patients with acute ischaemic stroke, using the ARI.[8] Interpreting this result in terms of the underlying pathology is difficult, given the nature of the ARI: the use of the model proposed here would enable more information to be gained from the experimental data. Also using the ARI, cerebral autoregulation has been shown to be preserved in both controls and in patients with recurrent vasovagal syncope only in the initial period after head-up tilt, declining in the syncopal group immediately before syncope.[3] However, using the frequency response, the cerebral autoregulation

of patients with neurally mediated syncope has been found to be preserved during the whole of the head-up tilt test, which lasted up to one hour.[24] By assessing the above experimental data with the model proposed here, however, more information could be learnt about the status of autoregulation than can be gained solely from the ARI.

It should be noted that the cerebral autoregulation system is more complicated than presented in this analysis: in particular only the linear dynamic behaviour has been examined here and experimental data presented by other authors[14] has seemed to indicate that the response may be heavily non-linear, especially in the low frequency range. The experimental data has been used to estimate more mathematically abstract models of the autoregulation, using first, second and third order kernels[5,14]: although the first order kernel has now been related to a physiologically-based model to provide a physiological interpretation, this is missing for the higher order kernels.

The presence of the one remaining degree of freedom in the model, however, means that it is not possible to determine all the necessary model parameters from just the IR. It would be valuable to find a means of obtaining more information experimentally to eliminate this degree of freedom. Since only non-invasive measurements are likely to be practical in most subjects, there are few extra experimental parameters available. However, one measurement technique that might have potential is Near Infra-Red Spectroscopy (NIRS), which can be used to measure changes in oxyhaemoglobin and deoxyhaemoglobin, both of which are flow dependent. Since there appears not to be any available experimental data for the transfer function between these two parameters and ABP, it is difficult to tell whether this is feasible. However, the model presented here could easily be extended to include the transport of haemoglobin and a theoretical analysis of this model would enable the potential of these measurements to be determined in assessing cerebral autoregulation, either on their own or in conjunction with V_{MCA} measurements. This will be the subject of future work.

CONCLUSIONS

In this paper the linear dynamic behaviour of the cerebral autoregulation system has been examined in detail, using a physiologically-based model which is analysed and compared to experimental data taken from the literature. The physiological model is based on a feedback mechanism with gain and time constant and is found to approximate very closely to a second order feedback system for the V_{MCA}/ABP transfer function. This shows very good agreement with experimental data and can thus be used to estimate the model parameters. A key advantage of this model is that the number of parameters to be estimated is close to the number of free variables. It is thus a compact model and its parameters can be derived robustly: a more complex model would have more degrees of freedom and would be harder to interpret from experimental data, whereas a simpler model would have too few degrees of freedom and provide less physiological insight.

Clearly the model is still an approximation to the underlying processes, but enables valuable clinical information to be gained from experimental data. The approach presented here is similar to that proposed by Tiecks,[25] but starting from a physiologically-based model, that enables the status of autoregulation to be interpreted in terms of a feedback gain and time constant, rather than a somewhat arbitrary difference equation. It would be extremely valuable to perform the parameter estimation process outlined here on a wide range of patient groups to examine whether the autoregulation status is different between the separate groups.

APPENDIX

To derive the linear transfer function, small changes about the basal conditions are assumed using a Taylor series expansion. Since the resulting equations will all be linear, the Laplace transform is used to convert the differential equations into a transfer function.

Equation (2) becomes:

$$\Delta R_{sa} = -2\frac{\Delta V_{sa}}{V_{sa}} R_{sa}. \tag{A1}$$

Equation (3) becomes:

$$s\Delta V_{sa} = sC_a\Delta p_1 + s\Delta C_a\,(p_1 - p_{ic})\,. \tag{A2}$$

Equations (4) and (7) combine to give:

$$sC_v\Delta p_2 = \frac{\Delta p_1 - \Delta p_2}{\left(R_{sa}/2 + R_{sv}\right)} - q\frac{\Delta R_{sa}/2}{\left(R_{sa}/2 + R_{sv}\right)} - \frac{\Delta p_2}{R_{lv}}. \tag{A3}$$

Equation (6) becomes:

$$s\Delta V_{sa} = \frac{\Delta p_a - \Delta p_1}{\left(R_{la} + R_{sa}/2\right)} - q\frac{\Delta R_{sa}/2}{\left(R_{la} + R_{sa}/2\right)} - \Delta q. \tag{A4}$$

Equations (8) and (10) combine to give:

$$\Delta C_a = -C_a G\frac{\Delta q}{q\,(1 + s\tau)}. \tag{A5}$$

Equation (9) becomes:

$$\Delta q = \frac{\Delta p_1 - \Delta p_2}{\left(R_{sa}/2 + R_{sv}\right)} - q\frac{\Delta R_{sa}/2}{\left(R_{sa}/2 + R_{sv}\right)}. \tag{A6}$$

The six Eqs. (A1)/(A6), can be used to eliminate the unwanted variables (ΔV_{sa}, ΔR_{sa}, ΔC_a, Δp_1, Δp_2) to derive

the expression in Eq. (11). The transfer function for V_{MCA} can be found from the flow rate:

$$V_{\mathrm{MCA}} = \frac{1}{A}\frac{p_a - p_1}{\left(R_{\mathrm{la}} + R_{\mathrm{sa}}/2\right)}. \tag{A7}$$

Hence for small changes:

$$\frac{\Delta V_{\mathrm{MCA}}}{V_{\mathrm{MCA}}} = \frac{\Delta p_a - \Delta p_1}{(p_a - p_1)} - \frac{\Delta R_{\mathrm{sa}}/2}{\left(R_{\mathrm{la}} + R_{\mathrm{sa}}/2\right)}, \tag{A8}$$

since area is assumed constant. This can then be calculated from the expressions in Eqs. (27)–(32).

ACKNOWLEDGMENTS

Stephen Payne was funded by the UK Research Councils Inter-Disciplinary Research Consortium (IRC) 'Medical Images and Signals.' Thanks are due to the other members of the IRC for profitable discussions and to the two anonymous reviewers for helpful suggestions.

REFERENCES

[1]Blaber, A. P., R. L. Bondar, F. Stein, P. T. Dunphy, P. Moradshahi, M. S. Kassam, and R. Freeman. Transfer function analysis of cerebral autoregulation dynamics in autonomic failure patients. *Stroke* 28:1686–1692, 1997.

[2]Carey, B. J., P. J. Eames, M. J. Blake, R. B. Panerai, and J. F. Potter. Dynamic cerebral autoregulation is unaffected by aging. *Stroke* 31:2895–2900, 2000.

[3]Carey, B. J., B. N. Manktelow, R. B. Panerai, and J. F. Potter. Cerebral autoregulatory responses to head-up tilt in normal subjects and patients with recurrent vasovagal syncope. *Circulation* 104:898–902, 2001.

[4]Chiu, C.-C., and S.-J. Yeh. Assessment of cerebral autoregulation using time-domain cross-correlation analysis. *Comp. Bio. Med.* 31:471–480, 2001.

[5]Chon, K. H., Y.-M. Chen, N.-H. Holstein-Rathlou, and V. Z. Marmarelis. Nonlinear system analysis of renal autoregulation in normotensive and hypertensive rats. *IEEE Trans. Biomed. Eng.* 45:342–353, 1998.

[6]Czosnyka, M., S. Piechnik, H. K. Richards, P. Kirkpatrick, P. Smielewski, and J. D. Pickard. Contribution of mathematical modeling to the interpretation of bedside tests of cerebrovascular autoregulation. *J. Neurol. Neurosurg. Psychiatry* 63:721–731, 1997.

[7]Dorf, R. C., and R. H. Bishop. Modern Control Systems. Prentice-Hall, 2000.

[8]Eames, P. J., M. J. Blake, S. L. Dawson, R. B. Panerai, and J. F. Potter. Dynamic cerebral autoregulation and beat to beat blood pressure control are impaired in acute ischaemic stroke. *J. Neurol. Neurosurg. Psychiatry* 72:467–473, 2002.

[9]Giller, C. A., and M. Mueller. Linearity and non-linearity in cerebral haemodynamics. *Med. Eng. Phys.* 25:633–646, 2003.

[10]Kirkham, S. K., R. E. Craine, and A. A. Birch. A new mathematical model of dynamic cerebral autoregulation based on a flow dependent feedback mechanism. *Physiol. Meas.* 22:461–473, 2001.

[11]Lee, S. P., T. Q. Duong, G. Yang, C. Iadecola, and S. G. Kim. Relative changes of cerebral arterial and venous blood volumes during increased cerebral blood flow: Implications for BOLD fMRI. *Magn. Reson. Med.* 45:791–800, 2001.

[12]Liu, Y., A. A. Birch, and R. Allen. Dynamic cerebral autoregulation assessment using an ARX model:comparative study using step response and phase shift analysis. *Med. Eng. Phys.* 25:647–653, 2003.

[13]Mitsis, G. D., and V. Z. Marmarelis. Modeling of nonlinear physiological systems with fast and slow dynamics: I. Methodology. *Ann. Biomed. Eng.* 30:272–281, 2002a.

[14]Mitsis, G. D., R. Zhang, B. D. Levine, and V. Z. Marmarelis. Modeling of nonlinear physiological systems with fast and slow dynamics: II. Application to cerebral autoregulation. *Ann. Biomed. Eng.* 30:555–565, 2002b.

[15]Myers, C. W., M. A. Cohen, D. L. Eckberg, and J. A. Taylor. A model for the genesis of arterial pressure Mayer waves from heart rate and sympathetic activity. *Auton. Neurosci.* 91:62–75, 2001.

[16]Narayanan, K., J. J. Collins, J. Hamner, S. Mukai, and L. A. Lipsitz. Predicting cerebral blood flow response to orthostatic stress from resting dynamics: Effects of healthy aging. *Am. J. Physiol.* 281:R716–722, 2001.

[17]Olufsen, M. S., A. Nadim, and L. A. Lipsitz. Dynamics of cerebral blood flow regulation explained using a lumped parameter model. *Am. J. Physiol.* 282:R611–622, 2002.

[18]Panerai, R. B. System identification of human cerebral blood flow regulatory mechanisms. *Cardiovascular Eng.* 4:59–71, 2004.

[19]Panerai, R. B., S. L. Dawson, and J. F. Potter. Linear and nonlinear analysis of human dynamic cerebral autoregulation. *Am. J. Physiol.* 277:H1089–H1099, 1999.

[20]Panerai, R. B., D. M. Simpson, S. T. Deverson, P. Mahony, P. Hayes, and D. H. Evans. Multivariate dynamic analysis of cerebral blood flow regulation in humans. *IEEE Trans. Biomed. Eng.* 47:419–423, 2000.

[21]Panerai, R. B., S. L. Dawson, P. J. Eames, and J. F. Potter. Cerebral blood flow velocity response to induced and spontaneous sudden changes in arterial blood pressure. *Am. J. Physiol.* 280:H2162–H2174, 2001.

[22]Panerai, R. B., P. J. Eames, and J. F. Potter. Variability of time-domain indices of dynamic cerebral autoregulation. *Physiol. Meas.* 24:367–381, 2003.

[23]Reinhard, M., T. Muller, B. Guschlbauer, J. Timmer, and A. Hetzel. Transfer function analysis for clinical evaluation of dynamic cerebral autoregulation—a comparison between spontaneous and respiratory-induced oscillations. *Physiol. Meas.* 24:27–43, 2003.

[24]Schondorf, R., R. Stein, R. Roberts, J. Benoit, and W. Cupples. Dynamic cerebral autoregulation is preserved in neurally mediated syncope. *J. Appl. Physiol.* 91:2493–2502, 2001.

[25]Tiecks, F. P., A. M. Lam, R. Aaslid, and D. W. Newell. Comparison of static and dynamic cerebral autoregulation measurements. *Stroke* 26:1014–1019, 1995.

[26]Ursino, M., and M. Giulioni. Quantitative assessment of cerebral autoregulation from transcranial Doppler pulsatility: A computer simulation study. *Med. Eng. Phys.* 25:655–666, 2003.

[27]Ursino, M., and C. A. Lodi. A simple mathematical model of the interaction between intracranial pressure and cerebral hemodynamics. *J. Appl. Physiol.* 82:1256–1269, 1997.

[28]Ursino, M., and C. A. Lodi. Interaction among autoregulation, CO2 reactivity, and intracranial pressure: a mathematical model. *Am. J. Physiol.* 274:H1715–H1728, 1998.

[29]Ursino, M., A. Ter Minassian, C. A. Lodi, and L. Beydon. Cerebral hemodynamics during arterial and CO2 pressure changes: in vivo prediction by a mathematical model. *Am. J. Physiol.* 279:H2439–2455, 2000.

[30]Vespa, P. What is the optimal threshold for cerebral perfusion pressure following traumatic brain injury? *Neurosurg. Focus* 15:Article 4, 2003.

[31]Zhang, R., J. H. Zuckerman, C. A. Giller, and B. D. Levine. Transfer function analysis of dynamic cerebral autoregulation in humans. *Am. J. Physiol.* 274:H233–H241, 1998.

[32]Zhang, R., J. H. Zuckerman, and B. D. Levine. Spontaneous fluctuations in cerebral blood flow: insights from extended-duration recordings in humans. *Am. J. Physiol.* 278:H1848–H1855, 2000.